frontiers in
MOLECULAR NEUROSCIENCE

ORIGINAL RESEARCH ARTICLE
published: 31 May 2012
doi: 10.3389/fnmol.2012.00068

Genetically encoded proton sensors reveal activity-dependent pH changes in neurons

Joseph V. Raimondo, Agnese Irkle, Winnie Wefelmeyer, Sarah E. Newey and Colin J. Akerman*

Department of Pharmacology, Oxford University, Oxford, UK

Edited by:
Daniele Arosio, Consiglio Nazionale delle Ricerche, Italy

Reviewed by:
Oleg Krishtal, Ukrainian Academy of Sciences, Ukraine
Hansen Wang, University of Toronto, Canada

***Correspondence:**
Colin J. Akerman, Department of Pharmacology, Oxford University, Mansfield Road, OX1 3QT, Oxford, UK.
e-mail: colin.akerman@pharm.ox.ac.uk

The regulation of hydrogen ion concentration (pH) is fundamental to cell viability, metabolism, and enzymatic function. Within the nervous system, the control of pH is also involved in diverse and dynamic processes including development, synaptic transmission, and the control of network excitability. As pH affects neuronal activity, and can also itself be altered by neuronal activity, the existence of tools to accurately measure hydrogen ion fluctuations is important for understanding the role pH plays under physiological and pathological conditions. Outside of their use as a marker of synaptic release, genetically encoded pH sensors have not been utilized to study hydrogen ion fluxes associated with network activity. By combining whole-cell patch clamp with simultaneous two-photon or confocal imaging, we quantified the amplitude and time course of neuronal, intracellular, acidic transients evoked by epileptiform activity in two separate *in vitro* models of temporal lobe epilepsy. In doing so, we demonstrate the suitability of three genetically encoded pH sensors: deGFP4, E^2GFP, and Cl-sensor for investigating activity-dependent pH changes at the level of single neurons.

Keywords: intracellular pH, pH sensors, genetic reporters, epilepsy, neural activity, deGFP4, E^2GFP, Cl-sensor

INTRODUCTION

Green fluorescent protein (GFP), derived from *Aequorea victoria*, has become one of the most popular fluorescent reporters for monitoring protein localization and gene expression (Tsien, 1998). This popularity stems from the fact that GFP is genetically encoded, enabling it to be targeted to particular cell types, subcellular compartments, or single proteins. Whilst its use as a simple label has been spectacularly successful, GFP's value as a biosensor is arguably just as important. For instance, protein engineering via targeted mutagenesis of GFP has resulted in variants sensitive to specific ion species, which are relevant to biological mechanisms. These include genetically encoded reporters of Ca^{2+}, Cl^-, and H^+ ion concentrations (Miyawaki et al., 1997; Kuner and Augustine, 2000; Bizzarri et al., 2006; Markova et al., 2008; Arosio et al., 2010; Zhao et al., 2011). The negative logarithm of H^+ ion concentration (pH) is a fundamental cellular parameter that is critical to a series of processes including cell division, metabolism, apoptosis, and cell migration (Opie, 1965; Denker and Barber, 2002; Putney and Barber, 2003; Abad et al., 2004). Within the nervous system, the control of pH has particular relevance for synaptic transmission and the modulation of network excitability (Drapeau and Nachshen, 1988; Tabb et al., 1992; Dulla et al., 2005). Whilst pH affects neuronal activity, neuronal activity itself can generate sizeable shifts in intracellular pH (Ahmed and Connor, 1980; Xiong et al., 2000). This reciprocal relationship means that tools to accurately measure hydrogen ion concentration are important for understanding the role pH plays during the evolution of both physiological and pathological network states. Although GFP-based pH indicators have gained popularity as a marker of synaptic release (Miesenböck, 1998), to our knowledge they have not been utilized to study intracellular hydrogen ion fluxes associated with network activity. Previous work investigating the effect of spiking activity and neuronal depolarization on intracellular pH has relied either on pH-sensitive microelectrodes or pH-sensitive fluorescent dyes (Rose and Deitmer, 1995; Xiong et al., 2000). Genetically encoded, GFP-based pH reporters offer several potential advantages over these techniques, including single-cell or subcellular targeting, enhanced spatial resolution, no fluorophore leakage and reduced interference with endogenous H^+ transport mechanisms (Gatto and Milanick, 1993; Bizzarri et al., 2009).

On this basis we set out to assess a number of genetically encoded pH sensors in terms of their ability to report absolute shifts in intracellular neuronal pH associated with heightened network activity. We chose two genetically encoded ratiometric pH reporters: "deGFP4" (Hanson et al., 2002) and "E^2GFP" (Bizzarri et al., 2006), as well as a pH-sensitive chloride indicator, "Cl-sensor" (Markova et al., 2008). With each reporter we quantified the amplitude and time course of neuronal, intracellular, acidic transients associated with epileptiform activity. Two *in vitro* models of epilepsy revealed that seizure-induced intracellular acidic transients are likely to be an order of magnitude larger than previous estimates, which were based upon measurements made across regions of tissue. Our findings demonstrate the utility of employing GFP-based, genetically encoded pH indicators for investigating activity-dependent pH changes at the single-cell level.

MATERIALS AND METHODS

SLICE PREPARATION AND DNA TRANSFECTION

Rat organotypic hippocampal slice cultures were prepared using a method similar to that described by Stoppini et al. (1991).

Briefly, 7-day-old male Wistar rats were killed in accordance with the UK Animals Scientific Procedures Act 1986. The brains were extracted and placed in cold (4°C) Geys Balanced Salt Solution (GBSS), supplemented with D-glucose (34.7 mM). All reagents were purchased from Sigma-Aldrich, unless stated. The hemispheres were separated and individual hippocampi were removed and immediately sectioned into 350 μm thick slices on a McIlwain tissue chopper. Slices were rinsed in cold dissection media, placed onto Millicell-CM membranes and maintained in culture media containing 25% EBSS, 50% MEM, 25% heat-inactivated horse serum, glucose, and B27 (Invitrogen). Slices were incubated at 36°C in a 5% CO_2 humidified incubator before transfection. To prevent excessive growth of glial cells, the antimitotic agent ARA-C (10 μM) was added to the culture media on day five or six in culture. Neurons were biolistically transfected after 5–6 days *in vitro* using a Helios Gene Gun (120 psi; Bio-Rad). The target DNA was either E^2GFP as part of pcDNA3-ClopHensor (generously provided by Daniele Arosio, University of Trento; Addgene plasmid #25938), deGFP4 in pEGFP-N1 (generously provided by Jim Remington, University of Oregon) or Cl-sensor in pEGFP-C1 (generously provided by Piotr Bregestovski, INMED, Marseille). 50 μg of target DNA was precipitated onto 25 mg of 1.6 μm diameter gold microcarriers and bullets generated in accordance with the manufacturer's instructions (Bio-Rad). This resulted in sparse transfection rates (typically less than 10 cells per slice) and recordings were performed 2–4 days post-transfection. At the time of recording therefore, transfected neurons were equivalent to postnatal day 14–17.

ELECTROPHYSIOLOGICAL RECORDINGS

Hippocampal slices were transferred to a recording chamber and continuously superfused with 95% O_2/5% CO_2 oxygenated artificial cerebro-spinal fluid (aCSF), warmed to 32–35°C. The composition of the "standard" aCSF was (in mM): NaCl (120), KCl (3), $MgCl_2$ (2), $CaCl_2$ (2), NaH_2PO_4 (1.2), $NaHCO_3$ (23), D-Glucose (11). The pH was adjusted to be between 7.35 and 7.40 using NaOH. Two seizure models were used: a "0 Mg^{2+} model" and a "0 Cl^- model." Seizures were induced either by switching bath perfusion of slices with normal aCSF to nominally Mg^{2+}-free aCSF (0 Mg^{2+} model: Mg^{2+} omitted from standard aCSF) or nominally Cl^- free aCSF (0 Cl^- model: NaCl, $MgCl_2$, and $CaCl_2$ of standard aCSF replaced with 120 mM sodium D-gluconate, 1 mM MgSO4, and 3 mM calcium D-gluconate, respectively). The 0 Mg^{2+} seizure model is a well-described *in vitro* model of epilepsy, which promotes excitation by removing the voltage dependent Mg^{2+} block on NMDA receptors (Anderson et al., 1986; Mody et al., 1987; Gutiérrez et al., 1999; Avoli et al., 2002). The 0 Cl^- model of seizures represents the first *in vitro* model of epilepsy reported in the literature and has since been widely utilized (Yamamoto and Kawai, 1967, 1968, 1969; Chamberlin and Dingledine, 1988; Avoli et al., 1990). It is mechanistically similar to the well-described seizure models that use pharmacological blockade of $GABA_A$Rs to reduce the efficacy of GABAergic inhibition (Hablitz, 1984; Straub et al., 1996). Removal of Cl^- from the aCSF has the added advantage of preventing potential Cl^- fluxes that may complicate pH measurements from the pH and Cl^- sensitive genetic reporters such as the Cl-sensor (Markova et al., 2008). Only data from seizures that were compatible with the imaging protocols (i.e., seizure duration < 100 s) were analyzed. Patch pipettes of 3–5 MΩ tip resistance were pulled from filamental borosilicate glass capillaries (1.2 mm outer diameter, 0.69 mm inner diameter; Harvard Apparatus Ltd), using a horizontal puller (Sutter P-97). The pipettes were filled with an internal solution containing (in mM): K-gluconate (130), NaCl (10), $CaCl_2$ (0.1333), $MgCl_2$ (2), EGTA (1), KCl (4), and HEPES (10). Osmolarity was adjusted to 290 mOsM and the pH was adjusted to 7.38 with KOH. Neurons were visualized under a 40×, water-immersion objective (Leica SP2 or Olympus BX51WI). Hippocampal CA1 or CA3 pyramidal neurons in close proximity to the transfected neuron of interest (<200 μm between somata) were targeted for whole-cell recordings. All recordings were made in current clamp mode using an Axopatch 1D or Axoclamp 2B amplifier (Axon Instruments). Data was acquired with WinWCP Strathclyde Whole-Cell Analysis software (V.3.9.7; University of Strathclyde) and later combined with pH imaging data during off-line analysis using MATLAB (MathWorks).

RECORDING INTRACELLULAR pH

Concurrent with electrophysiological recordings, the intracellular pH of a transfected CA1 or CA3 pyramidal neuron was measured using the following imaging techniques. For E^2GFP transfected neurons, imaging was performed using an upright Leica SP2 AOBS laser scanning confocal microscope equipped with a 40× water immersion objective (NA 0.8). Sequential excitation of E^2GFP at 458 and 488 nm was achieved with a multiline argon laser. Emitted fluorescence was detected between 500 and 550 nm using a single photomultiplier tube (PMT) at a constant voltage. To compensate for fluctuations in laser intensity, a custom built laser power sensor (sample rate 10 kHz) was used to record laser power output during imaging (Zucker and Price, 2001; Arosio et al., 2010) and the resulting data was used to correct fluorescence ratios offline.

For deGFP4 and Cl-sensor transfected neurons, imaging was performed using an Olympus FV300 confocal microscope (Olympus, Japan), custom-converted for two-photon imaging and equipped with a MaiTai-HP Ti:sapphire femtosecond pulsed laser (Newport Spectra-Physics, USA). Images were acquired on a PC using Fluoview software (version 5.0, Olympus, Japan). The two-photon system was mounted on an Olympus BX51 upright microscope equipped with a 40× water immersion objective (NA 0.80). Fluorescence was detected using two externally mounted PMTs (R3896, Hamamatsu, Japan). An excitation wavelength of 810 or 850 nm was used for deGFP4 or Cl-sensor, respectively. Emitted fluorescence from deGFP4 was separated using a dichroic mirror at 495 nm and filtered for detection by the two PMTs at 450–490 and 500–550 nm. Emitted fluorescence from Cl-sensor was separated using a dichroic mirror at 510 nm before being filtered for detection at 460–500 and 520–550 nm. Images were exported to the MATLAB environment where background was subtracted and fluorescence averaged within regions of interest selected from the soma of single neurons. Excitation or emission fluorescence ratios (R_{pH}) were converted to pH according to calibration curves collected for each construct.

pH CALIBRATION

Intracellular pH was controlled by equilibrating extra and intracellular ion concentrations using the K^+/H^+ exchanger nigericin (10 μM) and the Cl^-/OH^- exchanger tributyltinchloride in a high K^+ aCSF containing (in mM) potassium D-gluconate (123), HEPES (23), D-glucose (11), NaH_2PO_4 (1.2), MgSO4 (2), and calcium D-gluconate (2) (Boyarsky et al., 1988). pH was adjusted with small aliquots of NaOH and, to avoid CO_2 dependent pH buffering, aCSF was bubbled with 100% O_2. After each adjustment of pH, at least 15 min were allowed for intracellular and extracellular compartments to equilibrate. For each indicator, either an excitation (E^2GFP) or emission (deGFP4, Cl-sensor) fluorescence ratio (R) was measured at different intracellular pHs:

$$R = \frac{S_N}{S_D}$$

S_N and S_D are the numerator and denominator of the calculated fluorescence ratio, respectively. The formation of a 1:1 analyte-sensor complex results in an equilibrium described by the Grynkiewicz equation (Grynkiewicz et al., 1985; Arosio et al., 2010), which can be written as follows:

$$pH_i = pK_a + \log\left(\frac{R - R_A}{R_B - R}\right) + \log\left(\frac{S_{D,A}}{S_{D,B}}\right)$$

R_A and R_B are the values of R for the ratiometric indicator in its most acidic and basic forms, respectively. Likewise, $S_{D,A}$ and $S_{D,B}$ reflect S_D in its acidic and basic form. pK_a is the acid dissociation constant of the indicator. Calibration data was fitted using the following rearranged version of the above equation:

$$R = \frac{R_B 10^{pH - pK_A - \log\left(\frac{S_{D,A}}{S_{D,B}}\right)} + R_A}{1 + 10^{pH - K_A - \log\left(\frac{S_{D,A}}{S_{D,B}}\right)}}$$

This allowed the pK_a of each construct to be determined and pH_i to be calculated from measured fluorescence ratios (R) during subsequent experiments.

DATA ANALYSIS AND STATISTICS

Data analysis was performed using custom-made programs in the MATLAB environment. Some statistical analysis was also performed using GraphPad Prism version 5.0 (GraphPad Software). Data are reported as mean ± SEM.

RESULTS

DETECTING ACTIVITY-DEPENDENT CHANGES IN pH USING GENETIC REPORTERS

To investigate whether genetic reporters of pH can be used to detect the effect of neuronal network activity upon intracellular pH at a single-cell level, we combined whole-cell patch clamp recordings with simultaneous two-photon or single-photon confocal imaging in hippocampal brain slices (**Figure 1**). The intracellular pH of individual pyramidal neurons within the CA1 and CA3 regions was measured using one of three genetically encoded ratiometric pH sensors: E^2GFP (Bizzarri et al., 2006), deGFP4 (Hanson et al., 2002), or Cl-sensor (Markova et al., 2008), which were delivered by biolistic DNA transfection methods. Hyper-active network states were generated using seizure models that result in periods of synchronized neuronal discharges (see Materials and Methods). The effects upon neuronal activity were monitored by performing whole-cell current clamp recordings from nearby pyramidal neurons (<200 μm between somata). This provided precise information regarding seizure onset, offset, and intensity, without disrupting the physiology of the imaged neuron (**Figure 1C**). With this arrangement we found that seizure episodes were associated with marked acidic pH transients in neurons (see below). The acidic pH transient typically began at the onset of the seizure (**Figure 1C**) and pH continued to decrease before reaching a minimum at, or shortly following, the end of the seizure. The pH then recovered to baseline levels in the period between seizure events. Across slices and experiments the network events varied in terms of duration and the signal to noise of the pH measurements was sufficient to detect acidic transients associated with relatively brief periods of network activity (see example in **Figure 1C**).

CALIBRATING GENETICALLY ENCODED pH SENSORS IN HIPPOCAMPAL NEURONS

We first assessed the ability of each pH sensor to report steady-state pH under our imaging conditions. deGFP4, E^2GFP, and Cl-sensor showed robust expression in primary hippocampal neurons following biolistic transfection (**Figures 2A–C**). Each genetic reporter was calibrated by systematically varying extracellular pH in the presence of a proton-permeable ionophore, to achieve known intracellular pH values (see Materials and Methods). E^2GFP was used as a ratiometric pH indicator by excitation. The protein was excited sequentially via single-photon excitation at 458 and 488 nm, with emission collected between 500 and 550 nm using a single PMT. The ratio of fluorescence collected using the two excitation wavelengths ($R_{pH} = F_{488}/F_{458}$) was shown to depend on intracellular pH with a pKa of 7.56 (**Figure 2A**, right). deGFP4 was employed as a ratiometric pH indicator by emission. A two-photon laser at 810 nm was used to excite the protein, whilst emission was simultaneously recorded at 450–490 and 500–550 nm by two separate PMTs. The fluorescence ratio between these emission windows ($R_{pH} = F_{500-550}/F_{450-490}$) was found to be dependent upon intracellular pH with a pKa of 7.42 (**Figure 2B**, right). Cl-sensor was also utilized as a ratiometric pH indicator by emission. This reporter was excited at 850 nm, whilst emission was simultaneously recorded at 460–500 and 500–550 nm by two separate PMTs. Once again, the fluorescence ratio ($R_{pH} = F_{500-550}/F_{460-500}$) was strongly dependent upon intracellular pH, with a pKa of 7.73 (**Figure 2C**, right). Under our imaging conditions the noise associated with the pH signal was found to be different for the three reporters ($P < 10^{-7}$, One-Way ANOVA). Comparing the root mean square (RMS) noise of the intracellular pH signal under baseline conditions revealed that E^2GFP exhibited the least noise (RMS = 0.01 ± 0.001 pH), then Cl-sensor (RMS = 0.02 ± 0.001 pH), and deGFP4 exhibited the greatest signal noise (RMS = 0.04 ± 0.004 pH). Nevertheless, for all three pH indicators, the calibration curves presented in **Figure 2** allowed absolute neuronal pH to be determined from

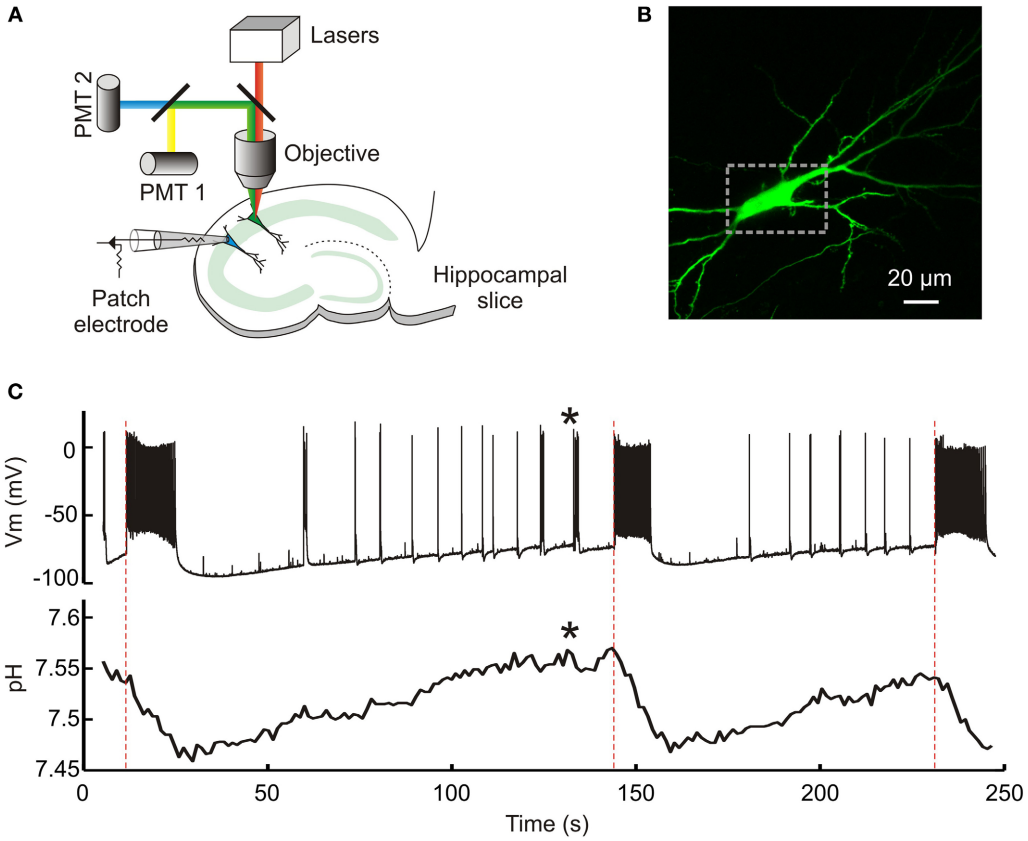

FIGURE 1 | Genetic reporters of pH detect intracellular pH changes during epileptiform activity. (A) A schematic of the experimental setup. A hippocampal pyramidal neuron transfected with a genetically encoded pH indicator was imaged using either two-photon or single-photon confocal microscopy. This allowed dynamic measurement of intracellular pH. A whole-cell patch recording from a neighboring neuron (cell somata <200 µm apart) provided simultaneous readout of seizure activity within the hippocampal slice. **(B)** A confocal image of a CA3 pyramidal neuron expressing the pH indicator E^2GFP. The dashed rectangle demarcates the region of interest used to estimate intracellular pH. **(C)** Dynamic intracellular pH measurements imaged from the neuron in "b" (lower trace). A neuron in close proximity was whole-cell patched and the membrane potential recorded over time in current clamp mode (upper trace). Perfusion of the slice with 0 Mg^{2+} induced periods of epileptiform activity characterized by membrane depolarization and high frequency firing, the onset of which is depicted by red dashed lines. Note the marked acidic shifts in pH that are associated with epileptiform activity. Even brief periods of activity were associated with detectable acidic transients (indicated by asterisks).

fluorescence ratios (R_{pH}), independent of protein expression levels.

GENETIC pH REPORTERS REVEAL ACIDIC INTRACELLULAR TRANSIENTS DURING 0 Mg^{2+} INDUCED EPILEPTIFORM ACTIVITY

Previous work using pH-sensitive electrodes or dyes has shown that neurons exhibit acidic shifts during heightened network activity (Rose and Deitmer, 1995; Xiong et al., 2000). Here we made use of pharmacological models of temporal lobe epilepsy to examine whether the ratiometric genetic reporters were able to capture dynamic shifts in pH during seizure activity. Omission of Mg^{2+} from the brain slice perfusate removes the voltage dependent Mg^{2+} block on NMDA receptors, which predisposes hippocampal slices to periods of synchronized hyperexcitability (Anderson et al., 1986; Mody et al., 1987; Gutiérrez et al., 1999; Avoli et al., 2002) and resulted in ictal-like seizure events of different durations (mean duration of analyzed seizures was 32.3 ± 1.6 s). Using this epilepsy model, we were able to demonstrate that the genetic pH reporters E^2GFP and deGFP4 are able to detect a highly significant negative shift in pH during epileptiform activity (E^2GFP: $P < 10^{-10}$, $n = 40$, deGFP4: $P < 10^{-7}$, $n = 19$, paired t test). As **Figures 3A,B** demonstrate, intracellular pH for CA3 pyramidal neurons decreases from baseline following the onset of epileptiform activity reaching a minimum at, or shortly following, seizure cessation. Neuronal pH then gradually re-alkalinizes to pre-seizure levels. To compare the pH responses recorded by the two pH reporters, we investigated the relationship between seizure length and the amplitude of maximum pH shift. When utilizing both E^2GFP and deGFP4 we observed a strong correlation between seizure duration and maximum pH change (E^2GFP: $r = -0.8270$, $P < 0.0001$, deGFP4: $r = -0.6056$, $P = 0.0060$, Pearson Correlation, **Figure 3C**). This relationship was indistinguishable for the two genetic reporters ($P = 0.4534$, Analysis of Covariance), which corroborated the magnitude of the pH shifts that were detected. As such, a linear fit could be applied to the pooled data from

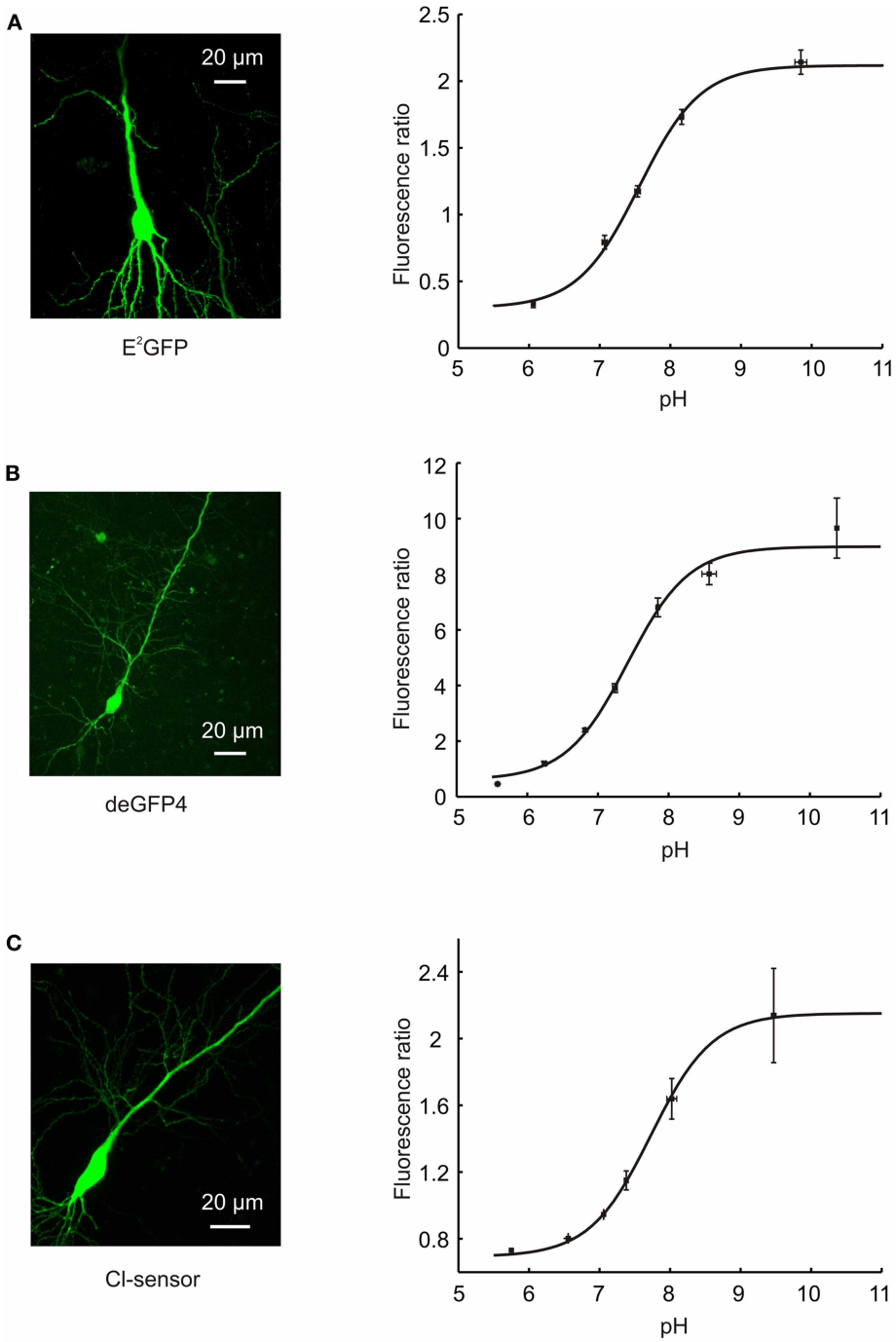

FIGURE 2 | Calibration of pH-sensitive GFP variants. (A) A confocal image of a hippocampal CA3 pyramidal neuron expressing E^2GFP (left). Calibration curve relating the fluorescence ratio of E^2GFP expressing neurons to their intracellular pH (right; $n = 4$). E^2GFP was used as an excitation ratiometric reporter, with excitation at two separate wavelengths (458 and 488 nm) and emitted light collected from a single window (500–550 nm). Intracellular pH was systematically varied by controlling extracellular pH in the presence of a proton-permeable ionophore (see Materials and Methods). Data was fit using established equations (Grynkiewicz et al., 1985; Arosio et al., 2010; see Materials and Methods) and pK_a was found to be 7.56. **(B)** A confocal image of a hippocampal CA3 pyramidal neuron expressing deGFP4 (left). Calibration curve relating the fluorescence ratio of deGFP4 expressing neurons to their intracellular pH (right; $n = 7$). deGFP4 was used as an emission ratiometric reporter, with excitation at a single wavelength (810 nm) and emission collected simultaneously at two separate windows (450–490 and 500–550 nm). The pH response properties of deGFP4 revealed a pK_a of 7.42. **(C)** A confocal image of a hippocampal CA1 pyramidal neuron expressing Cl-sensor (left). Calibration curve relating the fluorescence ratio of Cl-sensor expressing neurons to their intracellular pH (right; $n = 7$). Cl-sensor was used as an emission ratiometric reporter, with excitation at a single wavelength (850 nm) and emission collected simultaneously at two separate windows (460–500 and 520–550 nm). The pH response properties of Cl-sensor revealed a pK_a of 7.73.

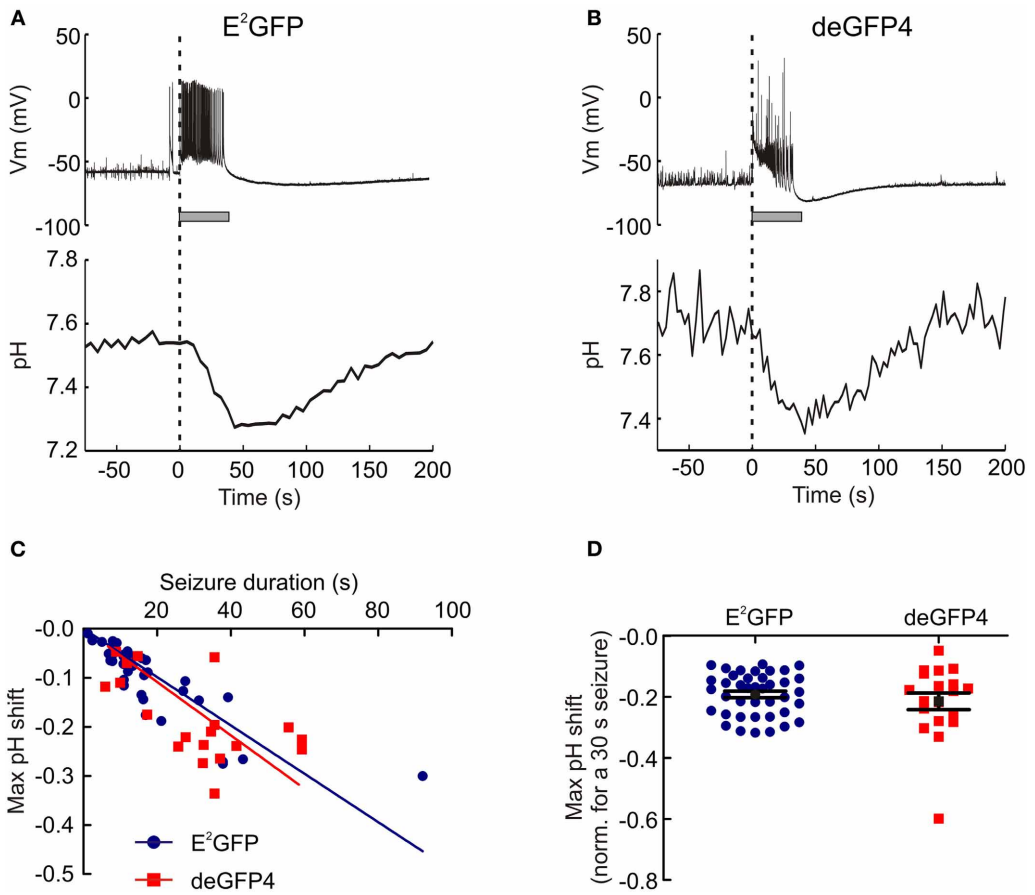

FIGURE 3 | 0 Mg^{2+} induced epileptiform activity induces acidic transients in neurons. (A) The intracellular pH of a hippocampal CA3 pyramidal neuron transfected with E^2GFP recorded during an episode of 0 Mg^{2+} induced epileptiform activity. The onset of epileptiform activity (dashed line) is correlated with the start of a decrease in intracellular pH. The pH continues to decrease during the seizure and reaches a minimum around the time of seizure termination (seizure duration is depicted by the horizontal gray bar), and then recovers to baseline in the post-seizure period. **(B)** Seizure-associated acidic transients of a similar amplitude were recorded from neurons expressing the pH reporter deGFP4. Although note the greater variance in the signal with this reporter. **(C)** The magnitude of intracellular acidic transients was directly proportional to seizure duration. This relationship was not dependent on the pH reporter used ($P = 0.4534$, Analysis of Covariance). **(D)** Maximum pH shifts normalized to a 30 s seizure had an average amplitude of 0.20 ± 0.1 pH units. This was not different for the two pH reporters ($P = 0.3581$, t test).

both probes and revealed a seizure-associated population shift of –0.005 pH units per second of seizure duration (**Figure 3C**). When the maximum pH shift from individual seizures was adjusted for a typical seizure duration of 30 s, the mean pH shift for E^2GFP neurons was -0.19 ± 0.01 ($n = 40$) and the mean pH shift for deGFP4 neurons was -0.21 ± 0.03 ($n = 19$) (**Figure 3D**).

GENETIC pH REPORTERS REVEAL ACIDIC INTRACELLULAR TRANSIENTS DURING 0 Cl^- INDUCED EPILEPTIFORM ACTIVITY

Having established the ability of genetically encoded reporters to show pH changes during 0 Mg^{2+} seizures, we were interested to test their performance in other models of hyper-excitability. $GABA_A$ receptors are primarily permeable to Cl^- (Hamill et al., 1983). Therefore, by removing Cl^- from the aCSF, one is able to profoundly reduce the efficacy of GABAergic inhibition (Yamamoto and Kawai, 1967, 1968, 1969; Chamberlin and Dingledine, 1988; Avoli et al., 1990) Removal of Cl^- from the aCSF has the added advantage of preventing potential Cl^- fluxes that may complicate pH measurements from the pH and Cl^- sensitive genetic reporter Cl-sensor (Markova et al., 2008). Using the 0 Cl^- seizure model we were able to demonstrate that the genetic pH reporters Cl-sensor and deGFP4 are also able to measure a highly significant negative shift in pH during epileptiform activity (Cl-sensor: $P < 10^{-22}$, $n = 40$, deGFP4: $P < 10^{-14}$, $n = 48$, paired t test). The pH response to 0 Cl^- seizure activity was qualitatively similar to that observed in response to 0 Mg^{2+} induced seizures, with activity causing an acidic transient that reached its maximum near the end of epileptiform episodes, before returning to baseline levels between seizure events (**Figures 4A,B**). Once again a strong relationship between seizure length and the size of maximum pH shift was apparent for both Cl-sensor and deGFP4 expressing neurons (Cl-sensor: $r = -0.5751$, $P = 0.0001$, deGFP4: $r = -0.4575$,

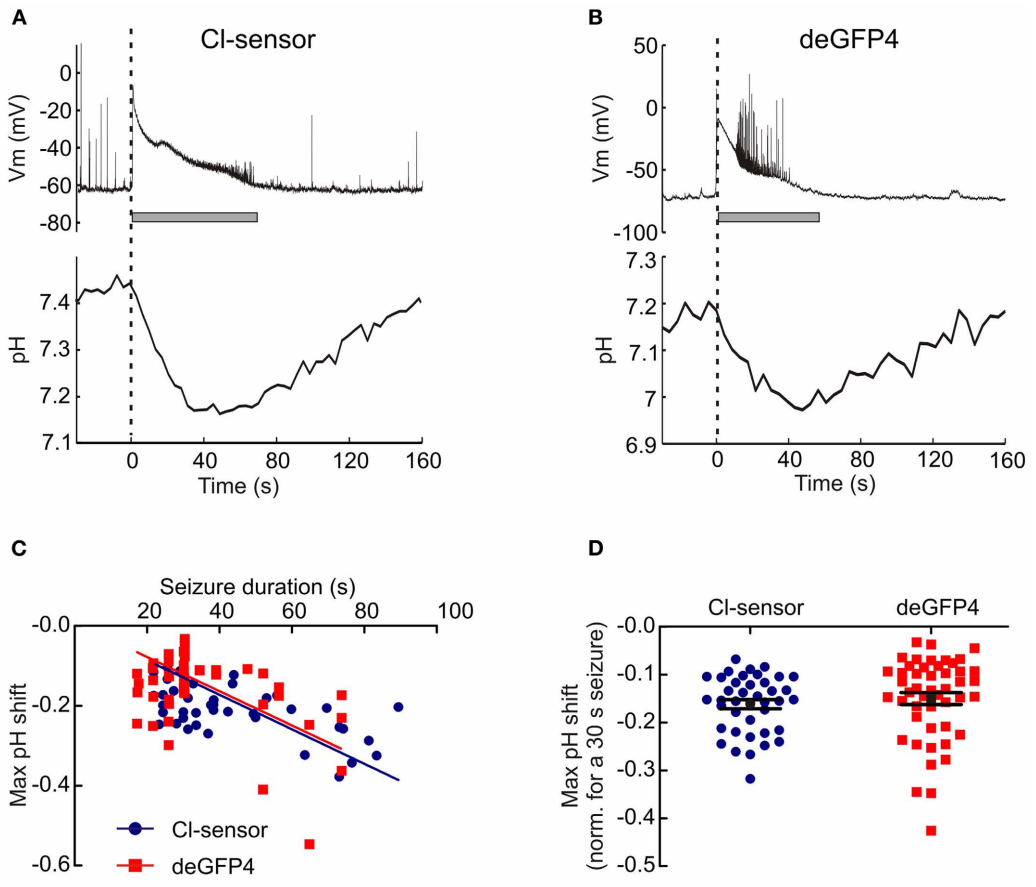

FIGURE 4 | 0 Cl^- induced epileptiform activity induces acidic transients in neurons. (A) The intracellular pH of a hippocampal CA1 pyramidal neuron transfected with Cl^- sensor recorded during an episode of 0 Cl^- induced epileptiform activity. Similar to the 0 Mg^{2+} model, the seizure onset (dashed line) is correlated with the start of a decrease in intracellular pH. The pH continues to decrease during the seizure, reaches a minimum around the time of seizure termination, and then recovers to baseline during the post-seizure period. **(B)** Similar acidic transients were associated with Cl^- induced epileptiform activity in neurons expressing the pH reporter deGFP4. **(C)** The magnitude of intracellular acidic transients was directly proportional to seizure duration. This relationship was not dependent on the pH reporter ($P = 0.2721$, Analysis of Covariance, Analysis of Covariance). **(D)** Maximum pH shifts normalized to a 30 s seizure had an average amplitude of 0.16 ± 0.1 pH units. This did not depend on the pH reporter being used ($P = 0.4726$, t test).

$P = 0.0011$, Pearson Correlation, **Figure 4C**). The relationship between seizure length and maximum pH shift was statistically indistinguishable for the two sensors ($P = 0.4534$, Analysis of Covariance), indicating that the values reported were accurate. And when a linear fit was applied to the pooled data this revealed a seizure-induced population shift of -0.0043 pH units per second of seizure (**Figure 4C**). When the maximum pH shift from individual seizures was adjusted for a seizure duration of 30 s, the mean pH shift for Cl-sensor neurons was -0.16 ± 0.01 ($n = 40$) and for deGFP4 neurons the mean was -0.15 ± 0.01 pH units ($n = 48$; **Figure 4D**).

GENETIC REPORTERS REVEAL DIFFERENCES IN THE KINETICS OF ACIDIC INTRACELLULAR TRANSIENTS

Having established the accuracy and sensitivity of the genetic pH reporters, we investigated whether they were able to detect differences in the kinetics of different seizures. We had observed that 0 Cl^- induced seizures tended to show a maximum depolarizing shift in the membrane potential at the onset of the seizure. In contrast, 0 Mg^{2+} induced seizures tended to reach maximal membrane depolarization at later stages of the seizure (**Figures 5A,B**). Indeed, across the population data the time of peak membrane potential depolarization relative to seizure duration occurred significantly earlier in 0 Cl^- ($27.0 \pm 1.3\%$ of seizure duration, $n = 88$) as compared to 0 Mg^{2+} seizures ($70.9 \pm 3.2\%$ of seizure duration, $n = 59$; $P < 0.0001$, t test, **Figure 5C**). To address whether these different seizure kinetics were associated with different intracellular pH dynamics we examined the timecourse of the acidic transients recorded, pooling data across the three genetic reporters. Consistent with the membrane potential measurements, we found that the time of the maximum pH shift occurred significantly earlier for 0 Cl^- seizures than for 0 Mg^{2+} seizures ($P = 0.0031$, t test, **Figure 5D**). In the case of 0 Cl^- the maximum acidic shift was reached at $109.7 \pm 3.2\%$ of seizure duration ($n = 88$),

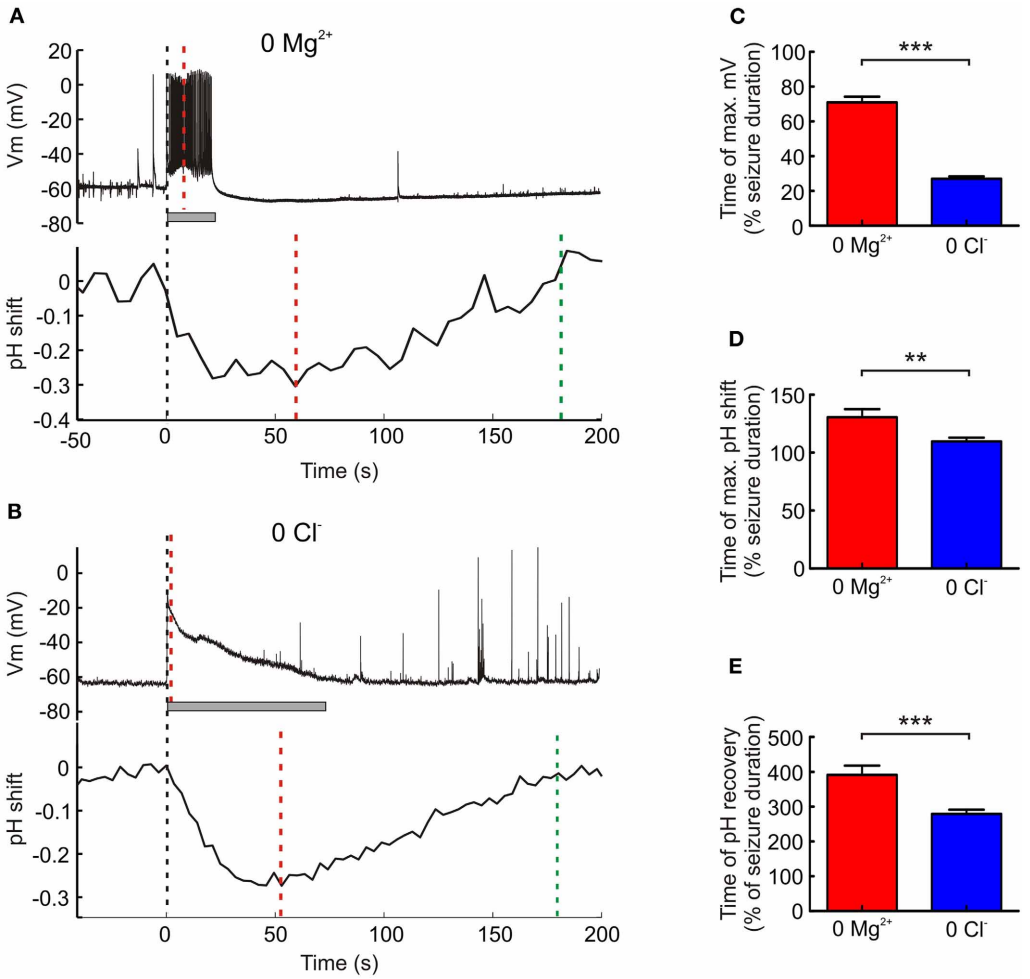

FIGURE 5 | The kinetics of acidic transients and epileptiform activity differ between seizure models. (A) The membrane potential (upper trace) of a hippocampal CA1 pyramidal neuron during a 0 Mg^{2+} induced seizure episode (seizure duration of 21 s, indicated by the gray bar). The membrane potential reaches its maximum (red dashed line) midway through the seizure. Simultaneous recording of a neighboring pyramidal neuron's intracellular pH (lower trace) reveals that this does not reach its minimum (red dashed line) until 35 s after the seizure terminates and recovers (green dashed line) by approximately 160 s following the end of the seizure. **(B)** The membrane potential (upper trace) of a CA1 pyramidal neuron during a 0 Cl^{-} induced seizure episode (seizure duration of 69 s, indicated by the gray bar). Unlike the 0 Mg^{2+} induced seizure, the membrane potential reaches its peak (red dashed line) almost immediately after the seizure begins. Simultaneous recording of a neighboring pyramidal neuron's intracellular pH (lower trace), reveals that the intracellular pH reaches its minimum (red dashed line) 23 s before the seizure ends and returns to baseline (green dashed line) approximately 105 s after the end of the seizure episode. **(C)** The time to reach maximum membrane depolarization as a percentage of seizure duration was significantly longer for 0 Mg^{2+} as opposed to 0 Cl^{-} induced seizures (***$P < 0.0001$, t test). **(D)** The time to reach maximum intracellular pH shift as a percentage of seizure duration was also significantly longer for 0 Mg^{2+} as opposed to 0 Cl^{-} induced seizures (**$P = 0.0031$, t test). **(E)** Similarly, the time of pH recovery as a percentage of seizure duration was significantly longer for 0 Mg^{2+} as compared to 0 Cl^{-} induced seizures (***$P < 0.0001$, t test).

whereas in the case of 0 Mg^{2+} the maximum acidic shift was reached at 130.5 ± 7.0% ($n = 59$) of seizure duration. Similarly, intracellular pH returned to baseline more rapidly in the 0 Cl^{-} model than the 0 Mg^{2+} model. pH recovered by 279.4 ± 12.1% of seizure duration following 0 Cl^{-} seizures ($n = 58$), whereas it required until 391.5 ± 26.7% of seizure duration to recover following 0 Mg^{2+} seizures ($n = 31$, $P < 0.0001$, t test, **Figure 5E**). These data are consistent with the timecourse of membrane depolarization recorded in the two epilepsy models (**Figure 5C**) and indicate that the genetic reporters are able to capture differences in the kinetics of activity-dependent pH changes.

DISCUSSION

We investigated the potential for genetically encoded pH reporters to measure neuronal intracellular pH transients associated with periods of elevated activity. Using a combination of patch clamp recordings and two-photon or single-photon confocal imaging in hippocampal brain slices, we assessed the performance of three different pH-sensitive fluorescent proteins. All three pH sensors were able to report acidic shifts associated with epileptiform activity, although there were differences in terms of their sensitivity, signal-to-noise and utility for activity-dependent studies. For our study we chose three ratiometric reporters of pH: E^2GFP, deGFP4,

and Cl-sensor (Hanson et al., 2002; Bizzarri et al., 2006; Markova et al., 2008). While a number of non-ratiometric GFP-derived pH indicators exist, these are susceptible to measurement artefacts caused by variations in excitation path length, indicator concentration, illumination stability, cell thickness, and indicator distribution (Hanson et al., 2002). In addition, non-ratiometric reporters cannot accurately record absolute pH without laborious within cell calibration. In contrast, ratiometric reporters overcome many of these issues. The genetically encoded ratiometric reporters can be classified into two groups, those that are constituted by a single GFP mutant and those that are a fusion of the pH-sensitive YFP with a less pH-sensitive GFP variant such as CFP (Bizzarri et al., 2009). The former group includes ratiometric pHlourin (RaGFP), deGFP4 and E^2GFP (Miesenböck, 1998; Hanson et al., 2002; Bizzarri et al., 2006). We utilised deGFP4 as it is the only ratiometric pH indicator that has been convincingly established for two-photon use (Hanson et al., 2002). E^2GFP was selected because it is optimally excited with wavelengths that are common to Argon-*ion* lasers, which facilitates its use with confocal microscopy. Under our conditions we found that deGFP4 and E^2GFP could report intracellular pH with a similar pK_a. However, data gathered using deGFP4 was considerably noisier, most likely due to the weak fluorescence emitted by deGFP4 in the blue wavelength range (Hanson et al., 2002). E^2GFP proved to be an excellent ratiometric indicator by excitation although, as is common to indicators used in this fashion, accurate intracellular pH recordings required us to measure and correct for independent power fluctuations associated with the two excitation laser lines (Arosio et al., 2010).

Reporters based upon YFP fusions include YFpH, pHlameleon, clomeleon, and Cl-sensor (Kuner and Augustine, 2000; Awaji and Hirasawa, 2001; Esposito et al., 2008; Markova et al., 2008). YFP fluorescence is quenched by both Cl^- and H^+ ions and, as a result, YFP fusion proteins are sensitive to both intracellular pH and Cl^- concentration (Jayaraman et al., 2000). This dual sensitivity complicates the interpretation of *in vivo* measurements using these probes, particularly as neuronal processes often involve either the related, or independent, flux of both Cl^- and H^+ ions (Tabb et al., 1992; Doyon et al., 2011). Attempts to reduce the Cl^- sensitivity of YFP by inducing mutations in the Cl^- binding pocket produced mutants with a low pK_a, that is less suited for physiological pH measurements (Griesbeck et al., 2001). We circumvented the issue of dual sensitivity by utilizing a Cl^- free model of epilepsy in order to test the pH sensitivity of the YFP fusion protein, Cl-sensor. This ensured that the activity-dependent fluctuations in fluorescence ratio we recorded could be attributed to changes in intracellular H^+ ion concentration. Under these specific conditions, Cl-sensor proved to be an excellent ratiometric pH indicator by emission, with a signal to noise ratio comparable to that of E^2GFP. This shows that Cl-sensor can be used as a reporter of intracellular pH dynamics and equally that the dual ion-sensitivity of this reporter (and presumably that of closely related YFP fusion proteins such as Clomeleon) should be considered when examining activity-dependent changes (Kuner and Augustine, 2000). One additional point is that despite employing two-photon excitation, pH measurements using Cl-sensor sometimes exhibited slow baseline drift, presumably as a result of the differential bleaching rates experienced by the YFP as opposed to the CFP fluorophore (Tramier et al., 2006; Bregestovski et al., 2009).

Previous studies investigating activity-dependent intracellular pH transients have employed either pH-sensitive microelectrodes or pH-sensitive dyes (Rose and Deitmer, 1995; Xiong et al., 2000). Due to their size, the use of microelectrodes to measure pH has been mostly confined to large neurons. pH-sensitive dyes meanwhile are widely used to report intracellular pH and several classes exist including fluoresceins, benzoxanthenes, rhodols, and pyrenes. The fluorescein derivatives, 2′-7′-bis (carboxyethyl)-5(6)-carboxyfluorescein (BCECF) and carboxyseminaphthorhodafluor- I (carboxy-SNARF-1) are by far the most popular. These two dyes are suitable for use as ratiometric pH indicators and have desirable optical properties. In addition, both dyes are available as acetoxymethyl (AM) esters, which facilitates intracellular loading without the use of micropipettes. However, fluorescein dyes have a potentially significant disadvantage, which may be particularly relevant to studies of activity-dependent proton fluxes within the nervous system. Fluorescein analogues have been shown to inhibit the Ca^{2+}/H^+ ATPase (Gatto and Milanick, 1993; Chesler, 2003). This ATP dependent transporter extrudes Ca^{2+} in exchange for H^+. As Ca^{2+} influx is a primary feature of neuronal membrane depolarization, the restoration of low Ca^{2+} via this exchanger is thought to be an important mechanism by which protons accumulate during neuronal activity (Schwiening et al., 1993; Svichar et al., 2011).

Employing three different genetically encoded pH indicators and two separate models of epilepsy we show that epileptiform activity lasting on the order of 30 s generates intracellular acidic shifts of between 0.1 and 0.3 pH units. This is an order of magnitude larger than previous estimates (Xiong et al., 2000), and there are several possible explanations for this difference. Firstly, in contrast to Xiong et al. who employed a non-synaptic Ca^{2+} free model of epileptiform activity, we utilized models that left the majority of synaptic transmission intact and either elevated synaptic excitation ($0\,Mg^{2+}$) or reduced synaptic inhibition ($0\,Cl^-$). As Ca^{2+} is known to accompany neuronal activity, the role of H^+ import via the Ca^{2+}/H^+ ATPase (see above) may contribute to the observed difference in acidic transient magnitude observed. Another factor is likely to be the differences in tissue imaging. Xiong and colleagues averaged fluorescence changes across regions of tissue, which presumably included different cell types and fluorescence from dye that is not exposed to pH changes. By restricting our imaging to individual hippocampal pyramidal neurons, the data from the genetic reporters should more accurately reflect the magnitude of seizure-induced intracellular acidic transients, at least in this cell type. It is also unknown whether differences in intracellular pH buffering power exogenously introduced by the separate reporters could explain the observed differences. Nonetheless, our observations suggest that the degree of acidification is more pronounced than previously appreciated and this should be considered in future studies of network activity and epilepsy.

Our simultaneous recordings also enabled us to assess the temporal properties of seizure-induced acidic transients in hippocampal pyramidal neurons. Consistent with previous work, we found that the time of maximum acidity correlated with seizure termination (Xiong et al., 2000). This is consistent with the idea that activity-dependent intracellular acidification may serve as a local feedback signal that dampens network excitability (Chesler, 2003). We were also able to detect differences in the temporal properties of pH shifts induced by the two separate seizure models. The 0 Mg^{2+} seizure model resulted in maximum pH shifts and recovery times that occurred relatively later than those induced by the 0 Cl^- seizure model. This most likely reflects the fact that following seizure onset, 0 Mg^{2+} seizures typically displayed a progressive increase in seizure intensity, whilst the 0 Cl^- seizures reached maximum depolarization almost immediately after the start of the seizure. These observations suggest that the pattern of neural activity is linked to the kinetics of pH changes and it will be interesting to explore this relationship in future studies.

The current study did not investigate the molecular mechanisms underlying seizure-induced acidification. It should also be noted that any measured change in pH during activity is necessarily a function of both the proton flux into the cell cytoplasm and its intracellular pH buffering capacity (Chesler, 2003). At least three major processes are likely to be involved in seizure-induced acidification. Firstly, as described earlier, a fall in pH is linked to the activity induced entry of Ca^{2+} due to the function of Ca^{2+}/H^+ ATPases located in the plasma membrane and endoplasmic reticulum (Schwiening et al., 1993; Makani and Chesler, 2010). Secondly, prolonged neural activity will increase the production of metabolic acids such as CO_2 and lactate (Wang et al., 1994). And thirdly, the intense $GABA_AR$ activation that accompanies seizure activity has been shown to result in considerable HCO_3^- efflux and a resulting intracellular acidification (Pasternack et al., 1993; Trapp et al., 1996). The relative contribution of these different acidification mechanisms in the two seizure models that we examined is uncertain, as are potential differences in intracellular buffering capacity. For instance, it is possible that longer periods of sustained high frequency action potential activity during 0 Mg^{2+} seizures may mean that Ca^{2+} entry and metabolic demand could be greater in this model of epileptiform activity. Meanwhile, as $HC0_3^-$ is the only ion that is able to traverse $GABA_ARs$ in the absence of Cl^-, acidification as a result of $HC0_3^-$ efflux may play a relatively more important role in eliciting acidic transients in the 0 Cl^- seizure model. This highlights that it will also be interesting to examine how the recruitment of different acidification mechanisms influences the kinetics of activity-dependent pH changes in neurons.

Although our study did not include measurement of pH shifts in the extracellular space, previous work has demonstrated that seizures and stimulated activity are associated with an initial extracellular alkaline shift followed by a prolonged acidosis (Caspers and Speckmann, 1972; Urbanics et al., 1978). Our study supports these observations in that the initial intracellular acid shift in neurons would be predicted to cause an extracellular alkalinisation as acid equivalents enter the cell, whilst the post-seizure recovery from acidosis would likely result in a prolonged extracellular acid transient. A small number of studies have also described a rapid extracellular acidic transient preceding the biphasic response described above (Krishtal et al., 1987). This is presumably due to vesicular protons released during synaptic transmission (DeVries, 2001), however a glial source of protons cannot be excluded (Grichtchenko and Chesler, 1994).

In summary, we demonstrate the utility of employing GFP-derived, genetically encoded pH reporters for quantifying intracellular pH in the context of changing neuronal activity. Future work may leverage the advantages of this technique to investigate potential differences in pH response dynamics according to different network states, activity patterns, cell type, and subcellular compartment.

ACKNOWLEDGMENTS

We thank Piotr Bregestovski (INMED, Marseille), Daniele Arosio (Instituto di Biofisica, University of Trento) and Jim Remington (University of Oregon) for providing DNA constructs. We also thank members of the Akerman lab for providing insightful comments and critically reading the manuscript. This work was supported by a grant from the Medical Research Council (G0601503) and the research leading to these results has received funding from the European Research Council under the European Community's Seventh Framework Programme (FP7/2007-2013), ERC grant agreement number 243273. Joseph V. Raimondo was supported by a Rhodes Scholarship, Winnie Wefelmeyer was supported by a Wellcome Trust Studentship and Sarah E. Newey was supported by a Royal Society Dorothy Hodgkin Fellowship.

REFERENCES

Abad, M. F. C., Di Benedetto, G., Magalhães, P. J., Filippin, L., and Pozzan, T. (2004). Mitochondrial pH monitored by a new engineered green fluorescent protein mutant. *J. Biol. Chem.* 279, 11521–11529.

Ahmed, Z., and Connor, J. A. (1980). Intracellular pH changes induced by calcium influx during electrical activity in molluscan neurons. *J. Gen. Physiol.* 75, 403–426.

Anderson, W. W., Lewis, D. V., Swartzwelder, H. S., and Wilson, W. A. (1986). Magnesium-free medium activates seizure-like events in the rat hippocampal slice. *Brain Res.* 398, 215–219.

Arosio, D., Ricci, F., Marchetti, L., Gualdani, R., Albertazzi, L., and Beltram, F. (2010). Simultaneous intracellular chloride and pH measurements using a GFP-based sensor. *Nat. Methods* 7, 516–518.

Avoli, M., D'Antuono, M., Louvel, J., Köhling, R., Biagini, G., Pumain, R., D'Arcangelo, G., and Tancredi, V. (2002). Network and pharmacological mechanisms leading to epileptiform synchronization in the limbic system *in vitro*. *Prog. Neurobiol.* 68, 167–207.

Avoli, M., Drapeau, C., Perreault, P., Louvel, J., and Pumain, R. (1990). Epileptiform activity induced by low chloride medium in the CA1 subfield of the hippocampal slice. *J. Neurophysiol.* 64, 1747–1757.

Awaji, T., and Hirasawa, A. (2001). Novel green fluorescent protein-based ratiometric indicators for monitoring pH in defined intracellular microdomains. *Biochem. Biophys. Res. Commun.* 289, 457–462.

Bizzarri, R., Arcangeli, C., Arosio, D., Ricci, F., Faraci, P., Cardarelli, F., and Beltram, F. (2006). Development of a novel GFP-based ratiometric

excitation and emission pH indicator for intracellular studies. *Biophys. J.* 90, 3300–3314.

Bizzarri, R., Serresi, M., Luin, S., and Beltram, F. (2009). Green fluorescent protein based pH indicators for *in vivo* use: a review. *Anal. Bioanal. Chem.* 393, 1107–1122.

Boyarsky, G., Ganz, M. B., Sterzel, R. B., and Boron, W. F. (1988). pH regulation in single glomerular mesangial cells. I. Acid extrusion in absence and presence of HCO^{3-}. *Am. J. Physiol.* 255, C844–C856.

Bregestovski, P., Waseem, T., and Mukhtarov, M. (2009). Genetically encoded optical sensors for monitoring of intracellular chloride and chloride-selective channel activity. *Front. Mol. Neurosci.* 2:15. doi: 10.3389/neuro.02.015.2009

Caspers, H., and Speckmann, E. (1972). Cerebral pO_2, pCO_2 and pH: changes during convulsive activity and their significance for spontaneous arrest of seizures. *Epilepsia* 13, 699–725.

Chamberlin, N. L., and Dingledine, R. (1988). GABAergic inhibition and the induction of spontaneous epileptiform activity by low chloride and high potassium in the hippocampal slice. *Brain Res.* 445, 12–18.

Chesler, M. (2003). Regulation and modulation of pH in the brain. *Physiol. Rev.* 83, 1183.

DeVries, S. H. (2001). Exocytosed protons feedback to suppress the Ca^{2+} current in mammalian cone photoreceptors. *Neuron* 32, 1107–1117.

Denker, S. P., and Barber, D. L. (2002). Cell migration requires both ion translocation and cytoskeletal anchoring by the Na-H exchanger NHE1. *J. Cell Biol.* 159, 1087–1096.

Doyon, N., Prescott, S. A., Castonguay, A., Godin, A. G., Kröger, H., and De Koninck, Y. (2011). Efficacy of synaptic inhibition depends on multiple, dynamically interacting mechanisms implicated in chloride homeostasis. *PLoS Comput. Biol.* 7:e1002149. doi: 10.1371/journal.pcbi.1002149

Drapeau, P., and Nachshen, D. A. (1988). Effects of lowering extracellular and cytosolic pH on calcium fluxes, cytosolic calcium levels, and transmitter release in presynaptic nerve terminals isolated from rat. *J. Gen. Physiol.* 91, 305–315.

Dulla, C. G., Dobelis, P., Pearson, T., Frenguelli, B. G., Staley, K. J., and Masino, S. A. (2005). Adenosine and ATP link PCO_2 to cortical excitability via pH. *Neuron* 48, 1011–1023.

Esposito, A., Gralle, M., Dani, M. A. C., Lange, D., and Wouters, F. S. (2008). pHlameleons: a family of FRET-based protein sensors for quantitative pH imaging. *Biochemistry* 47, 13115–13126.

Gatto, C., and Milanick, M. (1993). Inhibition of the red blood cell calcium pump by eosin and other fluorescein analogues. *Am. J. Physiol. Cell Physiol.* 264, C1577–C1586.

Grichtchenko, I., and Chesler, M. (1994). Depolarization-induced acid secretion in gliotic hippocampal slices. *Neuroscience* 62, 1057–1070.

Griesbeck, O., Baird, G. S., Campbell, R. E., Zacharias, D. A., and Tsien, R. Y. (2001). Reducing the environmental sensitivity of yellow fluorescent protein. Mechanism and applications. *J. Biol. Chem.* 276, 29188–29194.

Grynkiewicz, G., Poenie, M., and Tsien, R. Y. (1985). A new generation of Ca^{2+} indicators with greatly improved fluorescence properties. *J. Biol. Chem.* 260, 3440–3450.

Gutiérrez, R., Armand, V., Schuchmann, S., and Heinemann, U. (1999). Epileptiform activity induced by low Mg^{2+} in cultured rat hippocampal slices. *Brain Res.* 815, 294–303.

Hablitz, J. J. (1984). Picrotoxin-induced epileptiform activity in hippocampus: role of endogenous versus synaptic factors. *J. Neurophysiol.* 51, 1011–1027.

Hamill, O. P., Bormann, J., and Sakmann, B. (1983). Activation of multiple-conductance state chloride channels in spinal neurones by glycine and GABA. *Nature* 305, 805–808.

Hanson, G. T., McAnaney, T. B., Park, E. S., Rendell, M. E. P., Yarbrough, D. K., Chu, S., Xi, L., Boxer, S. G., Montrose, M. H., and Remington, S. J. (2002). Green fluorescent protein variants as ratiometric dual emission pH sensors. 1. Structural characterization and preliminary application. *Biochemistry* 41, 15477–15488.

Jayaraman, S., Haggie, P., Wachter, R. M., Remington, S. J., and Verkman, A. S. (2000). Mechanism and cellular applications of a green fluorescent protein-based halide sensor. *J. Biol. Chem.* 275, 6047–6050.

Krishtal, O. A., Osipchuk, Y. V., Shelest, T. N., and Smirnoff, S. V. (1987). Rapid extracellular pH transients related to synaptic transmission in rat hippocampal slices. *Brain Res.* 436, 352–356.

Kuner, T., and Augustine, G. J. (2000). A genetically encoded ratiometric indicator for chloride: capturing chloride transients in cultured hippocampal neurons. *Neuron* 27, 447–459.

Makani, S., and Chesler, M. (2010). Rapid rise of extracellular pH evoked by neural activity is generated by the plasma membrane calcium ATPase. *J. Neurophysiol.* 103, 667.

Markova, O., Mukhtarov, M., Real, E., Jacob, Y., and Bregestovski, P. (2008). Genetically encoded chloride indicator with improved sensitivity. *J. Neurosci. Methods* 170, 67–76.

Miesenböck, G. (1998). Visualizing secretion and synaptic transmission with pH-sensitive green fluorescent proteins. *Nature* 394, 192–195.

Miyawaki, A., Llopis, J., Heim, R., McCaffery, J. M., Adams, J. A., Ikurak, M., and Tsien, R. Y. (1997). Fluorescent indicators for calcium based on green fluorescent proteins and calmodulin. *Nature* 388, 883.

Mody, I., Lambert, J. D., and Heinemann, U. (1987). Low extracellular magnesium induces epileptiform activity and spreading depression in rat hippocampal slices. *J. Neurophysiol.* 57, 869–888.

Opie, L. (1965). Effect of extracellular pH on function and metabolism of isolated perfused rat heart. *Am. J. Physiol.* 209, 1075–1080.

Pasternack, M., Voipio, J., and Kaila, K. (1993). Intracellular carbonic anhydrase activity and its role in GABA-induced acidosis in isolated rat hippocampal pyramidal neurones. *Acta Physiol. Scand.* 148, 229–231.

Putney, L. K., and Barber, D. L. (2003). Na-H exchange-dependent increase in intracellular pH times G2/M entry and transition. *J. Biol. Chem.* 278, 44645–44649.

Rose, C. R., and Deitmer, J. W. (1995). Stimulus-evoked changes of extra- and intracellular pH in the leech central nervous system. II. Mechanisms and maintenance of pH homeostasis. *J. Neurophysiol.* 73, 132–140.

Schwiening, C. J., Kennedy, H. J., and Thomas, R. C. (1993). Calcium-hydrogen exchange by the plasma membrane Ca-ATPase of voltage-clamped snail neurons. *Proc. Biol. Sci.* 253, 285–289.

Stoppini, L., Buchs, P. A., and Muller, D. (1991). A simple method for organotypic cultures of nervous tissue. *J. Neurosci. Methods* 37, 173–182.

Straub, H., Köhling, R., Lücke, A., Fauteck, J.-D., Speckmann, E.-J., Moskopp, D., Wassmann, H., Tuxhorn, I., Wolf, P., Pannek, H., and Oppel, F. (1996). The effects of verapamil and flunarizine on epileptiform activity induced by bicuculline and low Mg^{2+} in neocortical tissue of epileptic and primary non-epileptic patients. *Brain Res.* 733, 307–311.

Svichar, N., Esquenazi, S., Chen, H.-Y., and Chesler, M. (2011). Preemptive regulation of intracellular pH in hippocampal neurons by a dual mechanism of depolarization-induced alkalinization. *J. Neurosci.* 31, 6997–7004.

Tabb, J., Kish, P., Van Dyke, R., and Ueda, T. (1992). Glutamate transport into synaptic vesicles. Roles of membrane potential, pH gradient, and intravesicular pH. *J. Biol. Chem.* 267, 15412–15418.

Tramier, M., Zahid, M., Mevel, J.-C., Masse, M.-J., and Coppey-Moisan, M. (2006). Sensitivity of CFP/YFP and GFP/mCherry pairs to donor photobleaching on FRET determination by fluorescence lifetime imaging microscopy in living cells. *Microsc. Res. Tech.* 69, 933–939.

Trapp, S., Luckermann, M., Brooks, P. A., and Ballanyi, K. (1996). Acidosis of rat dorsal vagal neurons *in situ* during spontaneous and evoked activity. *J. Physiol.* 496, 695–710.

Tsien, R. Y. (1998). The green fluorescent protein. *Annu. Rev. Biochem.* 67, 509–544.

Urbanics, R., Leniger-Follert, E., and Ltibbers, D. (1978). Time course of changes of extracellular H^+ and K^+ activities during and after direct electrical stimulation of the brain cortex. *Pflugers Arch.* 53, 47–53.

Wang, G. J., Randall, R. D., and Thayer, S. A. (1994). Glutamate-induced intracellular acidification of cultured hippocampal neurons demonstrates altered energy metabolism resulting from Ca^{2+} loads. *J. Neurophysiol.* 72, 2563–2569.

Xiong, Z. Q., Saggau, P., and Stringer, J. L. (2000). Activity-dependent intracellular acidification correlates with the duration of seizure activity. *J. Neurosci.* 20, 1290.

Yamamoto, C., and Kawai, N. (1967). Seizure discharges evoked *in vitro* in thin section from guinea pig hippocampus. *Science* 155, 341–342.

Yamamoto, C., and Kawai, N. (1968). Generation of the seizure discharge in thin sections from the guinea pig brain in chloride-free medium *in vitro*. *Jpn. J. Physiol.* 18, 620–631.

Yamamoto, C., and Kawai, N. (1969). Origin of the seizure discharge evoked *in vitro* in thin sections from the guinea pig dentate gyrus. *Jpn. J. Physiol.* 19, 119–129.

Zhao, Y., Araki, S., Wu, J., and Teramoto, T. (2011). An expanded palette of genetically encoded Ca^{2+} indicators. *Science* 557, 1888–1891.

Zucker, R. M., and Price, O. (2001). Evaluation of confocal microscopy system performance. *Cytometry* 44, 273–294.

Conflict of Interest Statement: The authors declare that the research was conducted in the absence of any commercial or financial relationships that could be construed as a potential conflict of interest.

Received: 30 March 2012; paper pending published: 20 April 2011; accepted: 13 May 2012; published online: 31 May 2012.

Citation: Raimondo JV, Irkle A, Wefelmeyer W, Newey SE and Akerman CJ (2012) Genetically encoded proton sensors reveal activity-dependent pH changes in neurons. Front. Mol. Neurosci. ***5****:68. doi: 10.3389/fnmol.2012.00068*